

UC San Diego

UC San Diego Previously Published Works

Title

Relationship of macular ganglion cell complex thickness to choroidal microvasculature drop-out in primary open-angle glaucoma

Permalink

<https://escholarship.org/uc/item/8f3816z8>

Journal

British Journal of Ophthalmology, 107(6)

ISSN

0007-1161

Authors

Micheletti, Eleonora

Moghimi, Sasan

El-Nimri, Nevin

et al.

Publication Date

2023-06-01

DOI

10.1136/bjophthalmol-2021-320621

Copyright Information

This work is made available under the terms of a Creative Commons Attribution License, available at <https://creativecommons.org/licenses/by/4.0/>

Peer reviewed

1 **Relationship of Macular Ganglion Cell Complex thickness to Choroidal**
2 **Microvasculature Dropout in Primary Open Angle Glaucoma**

3

4 Eleonora Micheletti^{1,2*}, Sasan Moghimi^{1*}, Nevin W. El-Nimri¹, Takashi Nishida¹, Min Hee
5 Suh³, James A. Proudfoot¹, Alireza Kamalipour¹, Linda M. Zangwill¹, Robert N. Weinreb¹

6

7 ¹ Hamilton Glaucoma Center, Shiley Eye Institute, Viterbi Family Department of
8 Ophthalmology, University of California San Diego, La Jolla, California

9 ² Department of Clinical and Surgical, Diagnostic and Pediatric Sciences, Section of
10 Ophthalmology, University of Pavia-IRCCS Fondazione Policlinico San Matteo, Pavia, Italy

11 ³ Department of Ophthalmology, Haeundae Paik Hospital, Inje University College of
12 Medicine, Busan, South Korea.

13

14 **Corresponding Author:** Robert N. Weinreb, MD, Shiley Eye Institute, University of
15 California, San Diego, 9500 Campus Point Drive, La Jolla, CA, 92093-0946, e-mail:
16 rweinreb@ucsd.edu, (858) 534-6290.

17 *These authors had equal contributions as co-first authors.

18

19

20

21 **Word count:** 3373

22

23

24

25

26 **ABSTRACT**

27 **Background/Aims:** To investigate the rate of ganglion cell complex (GCC) thinning in
28 primary open-angle glaucoma (POAG) patients with and without deep-layer
29 microvasculature dropout (MvD)

30 **Methods:** POAG patients who had at least 1.5 years of follow-up and a minimum of 3 visits
31 were included from the Diagnostic Innovations in Glaucoma Study. MvD was detected at
32 baseline by Optical Coherence Tomography angiography (OCT-A). Area and angular
33 circumference of MvD were evaluated on en-face choroidal vessel density images and
34 horizontal B-scans. Rates of global and hemisphere GCC thinning were compared in MvD
35 and non-MvD eyes using linear mixed-effects models.

36 **Results:** Thirty-six eyes with MvD and 37 eyes without MvD of 63 patients were followed
37 for a mean of 3.3 years. In 30 out of 36 eyes, MvD was localized in the inferotemporal
38 region. While mean baseline visual field mean deviation was similar between the two groups
39 ($p=0.128$), global GCC thinning was significantly faster in eyes with MvD than in those
40 without MvD (mean differences: -0.50 ($-0.83, -0.17$) $\mu\text{m}/\text{year}$; $P=0.003$). Presence of MvD,
41 area and angular circumference of MvD were independently associated with a faster rate of
42 thinning ($P=0.002$, $P=0.031$ and $P=0.013$, respectively).

43 **Conclusion:** In POAG eyes, GCC thinning is faster in eyes with MvD. Detection of MvD in
44 OCTA images can assist clinicians to identify patients who are at higher risk for central
45 macula thinning and glaucomatous progression and may require more intensive management.

46

47 **Key words:** Ganglion Cell Complex, Optical coherence tomography angiography, glaucoma,
48 glaucoma progression

49

50 **SYNOPSIS:**

- 51 In this observational cohort study, glaucomatous eyes with deep-layer microvascular dropout
- 52 (MvD) exhibited faster ganglion cell complex (GCC) thinning than those without MvD.

53 **INTRODUCTION**

54 Glaucoma is a chronic optic neuropathy characterized by progressive loss of retinal ganglion
55 cells (RGCs) associated with deterioration of retinal nerve fiber layer (RNFL) and optic nerve
56 head (ONH).[1] Among the multiple proposed mechanisms of optic nerve damage,
57 microvascular changes of the ONH have been proposed as a potential factor in the
58 development and progression of glaucoma.[2 3] The choroidal (or deep-layer)
59 microvasculature within the parapapillary area (PPA) may be of particular interest because it
60 mainly receives its blood supply by the short posterior ciliary arteries that also perfuse deep
61 ONH tissues.[4]

62 Several studies using optical coherence tomography angiography (OCT-A) have
63 demonstrated regional choroidal microvasculature dropout (MvD) in patients with
64 glaucoma,[4 5] which corresponds to a perfusion defect identified with indocyanine green
65 angiography.[6] The presence of MvD in glaucoma patients has been associated with
66 parameters of disease severity, such as a thinner retinal nerve fiber layer (RNFL) and worse
67 visual field (VF) mean deviation (MD).[4]

68 MvDs have been frequently found in the inferotemporal region within the beta zone of
69 parapapillary atrophy (β -PPA), the region consistent with the macula vulnerability zone
70 (MVZ); this corresponds to the superior paracentral VF area.[7] These findings suggested
71 that the impaired choroidal perfusion in the form of MvD might be associated with initial
72 parafoveal scotomas.[8] To our knowledge, there are no previous studies that focused on the
73 macular GGC layer to estimate its future changes in eyes with MvD. Early detection of such
74 macular structural damage is relevant to glaucoma management as the loss of central vision
75 can markedly impact patients' quality of life (QoL).[9] Prompt identification of these changes
76 may help the clinician to intensify their management to preserve a patient's QoL.[9 10]

77

78 The purpose of this study was to compare the rates of macular GCC thinning in glaucoma
79 eyes with and without MvD at baseline. We also examined whether area, angular
80 circumference (AC) and location of MvD were associated with more rapid changes of
81 macular GCC in glaucoma patients.

82

83 **MATERIALS AND METHODS**

84 **Participants**

85 This longitudinal study included POAG patients enrolled in Diagnostic Innovations in
86 Glaucoma Study (DIGS)[11 12] who underwent OCT-A (Angiovue; Optovue Inc., Fremont,
87 CA). All participants from DIGS who met the inclusion criteria described below were
88 included in the present study. Informed consent was obtained from all study participants. This
89 study received the institutional review board approval of the University of California, San
90 Diego (NCT00221897) and the methodology adhered to the tenets of the Declaration of
91 Helsinki. This study included eyes with a minimum of 3 macular OCT scans and a minimum
92 of 1.5 years of follow-up and a good quality baseline OCT-A ONH image.

93 Eyes were classified as glaucomatous if they had repeatable (at least 2 consecutive) abnormal
94 VF test results and evidence of glaucomatous optic neuropathy – defined as excavation, the
95 presence of focal thinning, notching of neuroretinal rim, or localized or diffuse atrophy of the
96 RNFL on the basis of masked grading of optic disc photographs by 2 graders. An abnormal
97 VF test was defined as a pattern standard deviation outside of the 95% normal confidence
98 limits or a Glaucoma Hemifield Test result outside normal limits.

99 Inclusion criteria also included (1) older than 18 years of age, (2) open angles on gonioscopy,
100 and (3) best-corrected visual acuity of 20/40 or better. Exclusion criteria included (1) history
101 of trauma or intraocular surgery (except for uncomplicated cataract surgery or glaucoma

102 surgery), (2) coexisting retinal disease, (3) uveitis, (4) non-glaucomatous optic neuropathy,
103 (5) axial length of 26 mm or more and (6) VF mean deviation (MD) <-8 dB at baseline.

104

105 **Optical Coherence Tomography Angiography (OCT-A)**

106 All participants underwent OCT-A and Spectral-Domain (SD)-OCT imaging using
107 AngioVue imaging system (OptoVue, Inc., Fremont, CA). This existing commercially
108 available SD-OCT platform provides both thickness and vascular measurements. With the
109 simultaneously acquired OCT and OCT-A volume of the AngioVue scan and automated
110 segmentation by the AngioVue software, thickness and vascular analyses can be derived from
111 the same image.

112 Macula 3 x 3 mm² scans (304 B-scans x 304 A-scans per B-scan) centered on the fovea and
113 ONH 4.5 x 4.5 mm² (304 B-scans x 304 A-scans per B-scan) centered on the ONH were
114 acquired with the AngioVue OCT-A system (software version 2018.1.0.43). The retinal
115 layers of each scan were segmented automatically by the AngioVue software.

116 For this study, whole en-face image vessel density (wiVD) and the en-face choroidal vessel
117 density map was derived from the entire 4.5 x 4.5 mm² scan that was centered on the ONH.

118 This en-face choroidal vessel density map contains layers below the retinal pigment
119 epithelium, including the choroid and sclera. The macula cube scanning protocol was used to
120 assess GCC thickness. GCC thickness regions of the whole image (wiGCC) were analyzed.

121 OCT-A and SD-OCT image quality review was completed according to the Imaging Data
122 Evaluation and Analysis Regarding Center standard protocol on all scans processed with
123 standard AngioVue software. Poor-quality images were excluded; these were defined as
124 images with 1) low scan quality with quality index (QI) of less than 4; 2) poor clarity; 3)
125 residual motion artifacts visible as irregular vessel pattern or disc boundary on the en-face

126 angiogram; 4) image cropping or local weak signal resulting from vitreous opacity; or 5)
127 segmentation errors that could not be corrected.

128

129 **Choroidal Microvasculature Dropout detection**

130 Dropout was required to be present in at least 4 consecutive horizontal B-scans and also to be
131 >200 μm in diameter in at least one scan and to be in contact with the OCT disc boundary.

132 The optic disc boundary was automatically detected by the Optovue software as the Bruch's
133 membrane/ RPE complex opening. In case of errors in disc demarcation, one trained observer
134 masked to the clinical information of the subjects corrected the disc boundary manually by
135 searching for the positioning of Bruch's membrane opening (BMO), as previously
136 described.[13]

137 Two observers (EM and NEN), who were masked to the clinical characteristics of the
138 participants, independently determined the presence or absence of MvD for each patient.
139 Disagreements between the 2 observers about the presence MvD were resolved by a third
140 adjudicator (SM).

141

142 **Measurement of MvD area, circumferential angle and location**

143 Optic disc and the PPA margins were detected by simultaneously viewing the stereoscopic
144 optic disc photographs and the scanning laser ophthalmoscopic (SLO) images that were
145 obtained along with the OCT-A images. MvD area was manually demarcated on en-face
146 choroidal vessel density maps using the line tool provided by ImageJ software (Version 1.53;
147 available at <http://imagej.nih.gov/ij/download.html>; *National Institute of Health, Bethesda,*
148 *Maryland, USA*). Littmann's formula was used to correct the ocular magnification in OCT-
149 A.[14 15] Details of the formula are provided elsewhere.[15] The Avanti SD OCT has a
150 default axial length of 23.95 mm and an anterior corneal curvature radius of 7.77 mm.

151

152 MvD angular circumference (AC) was measured as previously described.[16] In brief, the
153 two points at which the extreme borders of MvD area met the ONH border were identified
154 and defined as angular circumferential margins. The AC was then determined by drawing
155 two lines connecting the ONH center to the angular circumference margins of the MvD.
156 Both area and AC of the MvD were independently assessed by two trained graders who were
157 masked to the clinical data for each patient, including the GCC and RNFL thickness. Both
158 MvD area and angular circumference were defined as the mean of the measurements made by
159 the two observers to minimize interobserver variation.

160

161 MvD area that included large retinal vessels was included as part of the MvD area if the MvD
162 extended beyond the vessels. In cases where the retinal vessels were located at the border of
163 the MvD, the area covered by the vessels was excluded from the MvD area. Reflectance or
164 shadowing of the large vessels on the horizontal and en-face images were excluded from the
165 quantitative analysis by the two independent observers masked to the patients' baseline
166 characteristics. In an eye showing more than one MvD, the area and the angular extent of
167 each MvD were calculated separately and also added together to determine the total area and
168 the total angular extension of MvD for the eye.

169

170 The sectoral location of the dropout was determined based on the 8 separate sectors
171 corresponding to those on the RNFL vessel density map of the OCTA. For each MvD, a line
172 was drawn to equally bisect the angular circumferential margins of the MvD from the ONH
173 center, as previously reported,[17] to define the location of the MvD. Disagreements between
174 the 2 observers in determining the MvD location were adjudicated by the third experienced
175 grader.

176

177 **Statistical analysis**

178 Patient and eye characteristics data were presented as mean (95% confidence interval (CI))
179 for continuous variables and count (%) for categorical variables. Interobserver reproducibility
180 for the presence of MvD and for the measured MvD area and AC were assessed using k
181 statistics (i.e. k value) and interclass correlation coefficient (ICC), respectively. Categorical
182 variables were compared using the chi-square test. Mixed-effects modeling was used to
183 compare ocular parameters among groups. Mixed-effects modeling was used to compare
184 ocular parameters among groups. Evaluation of the effect of microvascular dropout (MvD)
185 on the mean rates of change in wiGCC was performed using a linear mixed model with
186 random intercepts and random slopes. In this model, the average values of the outcome
187 variables were explored using a linear function of time, and random intercepts and random
188 slopes were introduced with patient- and eye-specific deviations from this average value.
189 This model can account for the fact that different eyes may have different rates of wiGCC
190 thinning over time, while allowing for correlation between two eyes of the same individual.

191

192 Factors contributing to the rate of wiGCC were explored using linear mixed models. Potential
193 predictors which were associated with the rates of wiGCC thinning during the follow-up in
194 univariable analysis ($p < 0.1$) were included in the multivariable model. Statistical analyses
195 were performed using Stata version 16.0 (StataCorp, College Station, TX). P values of less
196 than 0.05 were considered statistically significant for all analyses.

197

198 **RESULTS**

199 Eighty-two POAG eyes of 69 patients met the eligibility criteria. Of these, 9 eyes of 6
200 patients were excluded because of the poor quality of their OCT-A images, resulting in

201 inclusion of 73 eyes of 63 (33 male and 30 female) POAG patients. Mean follow-up (95% CI)
202 was 3.3 (3.1, 3.5) years for both MvD and non-MvD eyes with an average of 4.2 (3.8, 4.7)
203 and 4.4 (4.0, 4.7) OCT visits, respectively (p=0.664).

204

205 Among the 73 eyes, MvD was observed in 36 (49.3%) eyes. In 16 (45%) of these 36 eyes,
206 MvD was located in the inferior region, whereas 15 eyes (42%) showed MvD in both inferior
207 and superior sectors. Interobserver agreement in detecting the presence of MvD (95% CI)
208 was excellent (kappa =0.92 (0.83, 1.00)). The intraclass correlation coefficient (ICC) for
209 interobserver reproducibility in measuring the area and the angular circumference of MvD
210 (95% CI) was 0.98 (0.97, 0.99) and 0.94 (0.90, 0.96), respectively.

211 **Figure 1** shows a representative case of the relationship between MvD at baseline and GCC
212 progressive thinning.

213

214 **Table 1** compares the demographics and clinical characteristics of eyes with and without
215 MvD. Mean age (95% CI) was 68.5 (65.1, 71.9) and 70.5 (66.9, 74.2) in the MvD group and
216 non-MvD group, respectively (P=0.437). Mean baseline VF MD (95%) was -2.8 dB (-3.6, -
217 2.0) and -2.1 dB (-2.7, -1.4) in the MvD eyes and non-MvD eyes, respectively (P=0.126).

218 The groups were similar in age, gender, race, axial length, CCT, baseline IOP, glaucoma
219 severity defined as VF MD and mean number of OCT follow-up visits. Disc hemorrhage was
220 detected in 8 (22%) MvD eyes and 4 (10.5%) non-MvD eyes (P=0.156). Mean baseline GCC
221 thickness (95% CI) was lower in the MvD group compared with the non-MvD group globally
222 (89.0 μ m (85.6, 92.4) vs. 94.1 μ m (90.7, 97.5), P= 0.041) and in the inferior hemifield
223 (P=0.003), but not in the superior hemifield (P=0.527).

Table 1. Characteristics of Eyes Categorized by Microvascular Dropout Group

Variables	MvD (+)	MvD (-)	P value
Characteristic	n=36 eyes of 30 patients	n=37 eyes of 33 patients	
Baseline age (years)	68.5 (65.1, 71.9)	70.5 (66.9, 74.2)	0.437
Gender (Female/ Male)	14/16	16/17	0.885
Race (African American/ Non-African American)	8/22	15/18	0.122
Self-reported hypertension, n (%)	21 (70.0)	20 (60.6)	0.435
Self-reported diabetes, n (%)	7 (23.3)	7 (21.2)	0.840
Axial length (mm)	24.2 (23.9, 24.5)	24 (23.7, 24.2)	0.181
CCT (μm)	534.0 (519.2, 548.8)	537.7 (525.2, 550.3)	0.694
Mean baseline IOP (mm Hg)	14.3 (12.9, 15.7)	15.0 (13.9, 16.1)	0.420
Mean IOP during follow-up (mm Hg)	14.5 (13.2, 15.8)	15.3 (14.1, 16.6)	0.360
Disease Severity by baseline 24-2 VF MD			0.155
Early glaucoma, Eye No. (%)	32 (88.9)	36 (97.3)	
Moderate and advanced glaucoma, Eye No. (%)	4 (11.1)	1 (2.7)	
MvD Location			
Inferior, Eye No. (%)	16 (45.7)		
Superior, Eye No. (%)	4 (11.4)		
Both hemispheres, Eye No. (%)	15 (42.9)		
Corrected MvD area (mm ²)	0.09 (0.04, 0.14)		
MvD angle (degree)	25.1 (15.3, 35.0)		
Disc hemorrhage, n (%)	8 (22.9)	4 (10.5)	0.156
Mean baseline VF MD (dB)	-2.8 (-3.6, -2.0)	-2.1 (-2.7, -1.4)	0.126

Mean baseline global GCC thickness (μm)	89.0 (85.6, 92.4)	94.1 (90.7, 97.5)	0.041
Mean baseline hemi-inferior GCC (μm)	86.5 (81.7, 91.3)	95.0 (91.9, 98.2)	0.003
Mean baseline hemi-superior GCC (μm)	91.1 (87.5, 94.8)	92.9 (88.9, 96.9)	0.527
Baseline cpRNFL thickness (μm)	75.6 (70.3, 81.0)	81.7 (77.2, 86.1)	0.056
Length of follow-up (years)	3.3 (3.1, 3.5)	3.3 (3.1, 3.5)	0.901
Number of OCTA visits	4.2 (3.8, 4.7)	4.4 (4.0, 4.7)	0.664

CCT = central corneal thickness; IOP = intraocular pressure; MD = mean deviation; MvD = microvascular dropout; VF = visual field. Values are shown in mean (95% confidence interval), unless otherwise indicated. Statistically significant P values are shown in bold.

224

225 **Table 2** and **Figure 2** shows the rate of thinning in global GCC and hemi-sectoral GCC in
 226 eyes with and without MvD. A significantly faster mean rate of GCC thinning in MvD eyes
 227 compared to non-MvD eyes was found in mean global, hemi superior, and hemi inferior area
 228 (mean difference (95% CI): -0.50 (-0.83, -0.17) $\mu\text{m}/\text{year}$; P=0.003, -0.55 (-0.92, -0.19)
 229 $\mu\text{m}/\text{year}$; P=0.003, and -0.48 (-0.84, -0.11) $\mu\text{m}/\text{year}$; P=0.010, respectively). Similar results
 230 were found after adjusting for confounding factors age, baseline VF MD and mean IOP
 231 during follow-up. These findings were also similar when adjusted for GCC thickness instead
 232 of baseline 24-2 VF MD.

233

Table 2. Comparison of Rates of Whole Image Ganglion Cell Complex Thinning between dropout and Non-dropout Eyes

	MvD Group	Non-MvD Group	Difference	P value
	Mean (95% CI)	Mean (95% CI)	Mean (95% CI)	(adjusted)
wiGCC Change Rate ($\mu\text{m}/\text{year}$)				
Mean Global	-1.35 (-1.59, -1.11)	-0.85 (-1.09, -0.62)	-0.50 (-0.83, -0.17)	0.003 (0.002)
Hemi Superior	-1.40 (-1.66, -1.14)	-0.85 (-1.10, -0.59)	-0.55 (-0.92, -0.19)	0.003 (0.004)
Hemi Inferior	-1.34 (-1.60, -1.08)	-0.87 (-1.12, -0.61)	-0.48 (-0.84, -0.11)	0.010

MvD = microvascular dropout; wiGCC = whole image ganglion cell complex. Values are shown in mean (95% confidence interval), unless otherwise indicated. Statistically significant P values are shown in bold.

*Adjusted to age, baseline 24-2 visual field mean deviation, and mean IOP.

234

235 Factors contributing to the rate of global GCC thinning during the follow-up are summarized
236 in **Tables 3**. Multivariable analysis showed that presence of MvD, area and AC of MvD and
237 mean IOP during follow-up were significantly associated with a faster rate of GCC thinning
238 (P=0.002, P=0.038, P=0.013 and P=0.020, respectively) after adjusting for age, baseline VF
239 MD and mean IOP during follow-up. These results were similar even after adjusting for
240 baseline GCC thickness instead of baseline 24-2 VF MD. Similar results were found after
241 including baseline IOP instead of mean IOP during follow-up (**Supplemental Table 1**).

Table 3. Factors Contributing to the Rate of Whole Image Ganglion Cell Complex Thinning Over Time by Univariable and Multivariable Mixed Model Analysis

Variables	Univariable Model		Multivariable Model 1		Multivariable Model 2		Multivariable Model 3	
	β , 95 % CI	P value	β , 95 % CI	P value	β , 95 % CI	P value	β , 95 % CI	P value
Age, per 10 years older	0.05 (-0.11, 0.21)	0.551	0.01 (-0.14, 0.15)	0.945	0.00 (-0.15, 0.15)	0.992	0.00 (-0.16, 0.15)	0.968
Gender: Male/Female	-0.20 (-0.55, 0.14)	0.247						
Race:								
African American/ Non-African American	0.01 (-0.35, 0.37)	0.959						
Self-reported diabetes	0.22 (-0.20, 0.64)	0.309						
Self-reported hypertension	-0.04 (-0.40, 0.33)	0.848						
Axial length, per 1mm longer	0.11 (-0.09, 0.30)	0.294						
CCT, per 100 μ m thinner	0.20 (-0.24, 0.64)	0.379						
Baseline IOP, per 1 mm Hg higher	-0.04 (-0.09, 0.00)	0.077						

Mean IOP during follow-up, per 1 mm Hg higher	-0.05 (-0.09, 0.00)	0.032	-0.05 (-0.10, -0.01)	0.012	-0.05 (-0.09, -0.01)	0.026	-0.05 (-0.10, -0.01)	0.020
Baseline VF MD, per 1 dB worse	-0.07 (-0.16, 0.01)	0.082	-0.05 (-0.12, 0.03)	0.243	-0.05 (-0.13, 0.03)	0.201	-0.04 (-0.12, 0.04)	0.292
Baseline VF PSD, per 1 dB worse	0.01 (-0.07, 0.08)	0.858						
Follow-up period, per 1 year longer	0.13 (-0.16, 0.41)	0.387						
OCT number of scans	0.09 (-0.04, 0.22)	0.185						
Presence of MvD	-0.50 (-0.83, -0.17)	0.003	-0.49 (-0.81, -0.18)	0.002				
Corrected MvD area, per 1 mm ² larger	-0.99 (-1.85, -0.14)	0.022			-0.92 (-1.75, -0.08)	0.031		
MvD angle, per 10 degrees wider	-0.01 (-0.01, 0.00)	0.009					-0.05 (-0.09, -0.01)	0.013

CCT = central corneal thickness; IOP = intraocular pressure; MD = mean deviation; MvD = microvascular dropout; OCT = optical coherence tomography; VF = visual field.

Values are shown in β coefficient (95% confidence interval). Statistically significant P values are shown in bold. Multivariable Model 1: presence of MvD; Multivariable Model 2: corrected MvD area; Multivariable Model 3: MvD angular circumference

244 **DISCUSSION**

245 This study showed that, with more than 3 years of follow-up, the rates of progressive GCC
246 thinning were significantly faster in eyes with MvD compared to non-MvD eyes, supporting
247 the role of MvD as a predictor of glaucoma progression. Furthermore, larger areas and
248 angular extensions of MvD showed faster rates of GCC loss when compared to eyes with
249 smaller MvDs. These findings demonstrate a possible role for OCT-A choroidal vessel
250 density assessment as a biomarker for predicting glaucomatous GCC thinning.

251

252 Previous studies revealed a significant association between MvD and other predictors of
253 glaucoma progression, such as lamina cribrosa defects[18-21] and disc hemorrhage
254 (DH).[22-25] Park et al. reported that MvD was topographically related to DH, and was also
255 associated RNFL thinning.[26] Evidence of DH during the follow-up of glaucoma eyes has
256 been reported as a relevant prognostic factor for accelerated central VF progression.[27]

257 As MvD was measured in the choroidal layer, it largely represents a localized perfusion
258 defect of the choriocapillaris and choroidal microvasculature in the β -PPA region, and may
259 indicate impaired perfusion of deep-layer tissues of the prelaminar or laminar region of the
260 ONH. Since IOP-independent factors, such as vascular insufficiency to the ONH, may play
261 an important role in the prognosis of OAG[2], MvD may be associated with accelerated
262 glaucoma progression. Indeed, higher rates of VF loss have been observed in MvD eyes
263 compared to those without MvD, despite no significant differences in IOP between the two
264 groups.[28] A recent study also showed that the presence of MvD was one of the strongest
265 predictive factors for faster progressive RNFL thinning over 2.5 years of follow-up.[29]

266

267 In the present study, eyes with MvD showed faster GCC thinning compared to non-MvD
268 eyes over more than 3 years of follow-up. In agreement with these findings, previous

269 investigators demonstrated a significant association between faster rate of central VF loss and
270 MvD detected during follow-up, whereas the rates of VF progression in the peripheral VF
271 region did not differ significantly between MvD and non-MvD groups.[28] In this earlier
272 study, the progression rate of VF was faster in the superior than in the inferior 10° zone,
273 suggesting that the location of MvD in the inferior areas might be topographically related to
274 poor prognosis during the course of the disease.

275

276 Several hypotheses may explain the faster rate of central macula thinning in eyes with
277 evidence of MvD. The large majority of the eyes showed MvD located in the inferotemporal
278 (IT) area rather than in other regions, a location consistent with the macular vulnerability
279 zone (MVZ) in the retina,[7] where most of the retinal ganglion cell axons from inferior
280 macular region project. Moreover, the most common pattern of GCC thinning in glaucoma is
281 the widening of an existing defect, followed by deepening.[30] Because GCC progression
282 reflects the expansion or deepening of a pre-existing initial GCC defect in eyes with MvD,
283 the rate of GCC thinning is likely to be faster in eyes with MvD than without it. Another
284 explanation is that parafoveal scotoma and central macula thickness involvement in patients
285 with early glaucoma are often associated with risk factors closely related to vascular
286 dysregulation in the ONH tissues, such as hypotension, migraine, and disc hemorrhage.[27]
287 As a consequence, eyes with signs of hypoperfusion to the ONH, such as those with MvD,
288 may show a faster rate of GCC thinning compared to eyes without MvD.

289 Baseline macular GCC thickness of the inferior hemifield was shown to be predictive of
290 central and peripheral VF progression in POAG.[31-33] Of note, the involvement of the
291 central 10° of the VF has been strongly correlated with vision-related QoL.[9] Daily
292 activities, such as walking, reading and driving, are more likely to be affected by initial
293 parafoveal VF defects compared to initial arcuate defects in glaucoma patients. Given the

294 substantial impact of central VF on quality of life, meticulous assessment of the
295 glaucomatous macular damage is recommended in imagining glaucoma patients with MvD.

296

297 In the present study, baseline inferior hemifield GCC was significantly thinner in the MvD
298 eyes compared with non-MvD eyes, and MvD was mostly localized in the IT sector (7-8
299 o'clock). These relationships support the possibility of a common mechanism between the
300 macular thinning and the choroidal vascular impairment. The rates of GCC thinning were
301 significantly faster in the eyes with MvD in both superior and inferior hemifields compared
302 to the non-MvD groups in this study. Similar results were shown by Lee et al., who reported
303 faster rates of superior and inferior RNFL thinning in eyes with MvD in both superior and
304 inferior hemispheres.[34]

305

306 It remains unclear whether the extent (the area and circumference) of MvD is associated with
307 the rate of glaucomatous damage. Whereas some retrospective studies[17 35] found that the
308 extent of MvD was positively associated with severity and rapid progression of VF loss, the
309 area of MvD at baseline was not significantly associated with faster rate of RNFL thinning in
310 the study by Kim et al.[16] In the present study, area and angular circumference of MvD at
311 baseline were significantly associated with the rate of future GCC thinning, suggesting that
312 the extent of MvD may represent an indicator of high-risk glaucoma patients.

313

314 Our study had several limitations. First, MvD size was measured on the en-face choroidal
315 vessel density map, which itself is subject to many limitations. To minimize subjectivity in
316 the measurement of MvD. We defined MvD as a complete loss of the choroidal
317 microvasculature with a size of 200 micron or greater in diameter, a method that has been
318 validated in previous studies.[19] In addition, large overlying retinal vessels or DHs may

319 project onto en-face choroidal vessel density images, and may induce projection artifacts or
320 shadows or make it difficult to detect or define MvD boundaries. In order to reduce these
321 potential false negatives, MvD was defined by 3 trained examiners using both en-face and B-
322 scan images and we found an excellent interobserver agreement ($k=0.935$) between graders.
323 Second, subjects with advanced stages of glaucoma (i.e. eyes with baseline MD <-8 dB) were
324 excluded. Thus, our results may not be generalizable to eyes with more advanced glaucoma.
325 Third, MvD area and AC were measured on en-face images using the automatic demarcation
326 of the BMO, and this was not accurately demarcated in some eyes. To overcome this
327 limitation, disc margin errors were manually corrected before the quantitative analysis of
328 MvD by a trained observer who was masked to the clinical characteristic of the subjects.
329 Fourth, the en-face choroidal vessel density image was used to detect MvD. Although this
330 slab includes both choroid and inner sclera, the choroid is not segmented specifically and one
331 cannot assume that it represents only the choroidal layer. Finally, ocular magnification effects
332 associated with axial length might have influenced MvD area as measured by OCT-A.
333 However, eyes with axial length > 26 mm were excluded in the current study. Moreover,
334 Littmann's formula was used to correct the magnification effect.

335

336 In conclusion, MvD is an independent predictor for accelerated GCC loss in eyes with
337 glaucoma, especially in early stages of the disease. The rate of GCC thinning was faster in
338 eyes with evidence of MvD and thinner GCC at baseline. The rate of GCC thinning was
339 significantly higher in both superior and inferior regions and the extent of MvD was also
340 associated with the rate of GCC thinning in the future. Especially with early POAG, these
341 findings suggest that assessment of MvD is useful for detection of patients at a high risk of
342 rapid progression who require more intensive observation and treatment.

343

344 **REFERENCES**

- 345 1. Weinreb RN, Aung T, Medeiros FA. The pathophysiology and treatment of glaucoma: a
346 review. *JAMA* 2014;311(18):1901-11.
- 347 2. Weinreb RN. Ocular blood flow in glaucoma. *Can J Ophthalmol* 2008;43(3):281-3.
- 348 3. Flammer J, Orgul S, Costa VP, et al. The impact of ocular blood flow in glaucoma. *Prog*
349 *Retin Eye Res* 2002;21(4):359-93.
- 350 4. Suh MH, Na JH, Zangwill LM, Weinreb RN. Deep-layer Microvasculature Dropout in
351 Preperimetric Glaucoma Patients. *J Glaucoma* 2020;29(6):423-28.
- 352 5. Akagi T, Iida Y, Nakanishi H, et al. Microvascular Density in Glaucomatous Eyes With
353 Hemifield Visual Field Defects: An Optical Coherence Tomography Angiography
354 Study. *Am J Ophthalmol* 2016;168:237-49.
- 355 6. Lee EJ, Lee KM, Lee SH, Kim TW. Parapapillary Choroidal Microvasculature Dropout in
356 Glaucoma: A Comparison between Optical Coherence Tomography Angiography and
357 Indocyanine Green Angiography. *Ophthalmology* 2017;124(8):1209-17.
- 358 7. Hood DC, Raza AS, de Moraes CG, Liebmann JM, Ritch R. Glaucomatous damage of the
359 macula. *Prog Retin Eye Res* 2013;32:1-21.
- 360 8. Lee EJ, Kim TW, Kim JA, Kim JA. Central Visual Field Damage and Parapapillary
361 Choroidal Microvasculature Dropout in Primary Open-Angle Glaucoma.
362 *Ophthalmology* 2018;125(4):588-96.
- 363 9. Prager AJ, Hood DC, Liebmann JM, et al. Association of Glaucoma-Related, Optical
364 Coherence Tomography-Measured Macular Damage With Vision-Related Quality of
365 Life. *JAMA Ophthalmol* 2017;135(7):783-88.
- 366 10. Kim JH, Rabiolo A, Morales E, et al. Risk Factors for Fast Visual Field Progression in
367 Glaucoma. *Am J Ophthalmol* 2019;207:268-78.

- 368 11. Sample PA, Girkin CA, Zangwill LM, et al. The African Descent and Glaucoma
369 Evaluation Study (ADAGES): design and baseline data. *Arch Ophthalmol*
370 2009;127(9):1136-45.
- 371 12. Girkin CA, Sample PA, Liebmann JM, et al. African Descent and Glaucoma Evaluation
372 Study (ADAGES): II. Ancestry differences in optic disc, retinal nerve fiber layer, and
373 macular structure in healthy subjects. *Arch Ophthalmol* 2010;128(5):541-50.
- 374 13. Zang P, Gao SS, Hwang TS, et al. Automated boundary detection of the optic disc and
375 layer segmentation of the peripapillary retina in volumetric structural and
376 angiographic optical coherence tomography. *Biomed Opt Express* 2017;8(3):1306-18.
- 377 14. Aykut V, Oner V, Tas M, Iscan Y, Agachan A. Influence of axial length on peripapillary
378 retinal nerve fiber layer thickness in children: a study by RTVue spectral-domain
379 optical coherence tomography. *Curr Eye Res* 2013;38(12):1241-7.
- 380 15. Bennett AG, Rudnicka AR, Edgar DF. Improvements on Littmann's method of
381 determining the size of retinal features by fundus photography. *Graefes Arch Clin Exp*
382 *Ophthalmol* 1994;232(6):361-7.
- 383 16. Kim JA, Lee EJ, Kim TW. Evaluation of Parapapillary Choroidal Microvasculature
384 Dropout and Progressive Retinal Nerve Fiber Layer Thinning in Patients With
385 Glaucoma. *JAMA Ophthalmol* 2019;137(7):810-16.
- 386 17. Lee JY, Shin JW, Song MK, Hong JW, Kook MS. An Increased Choroidal
387 Microvasculature Dropout Size is Associated With Progressive Visual Field Loss in
388 Open-Angle Glaucoma. *Am J Ophthalmol* 2021;223:205-19.
- 389 18. Lee SH, Kim TW, Lee EJ, Girard MJA, Mari JM. Focal lamina cribrosa defects are not
390 associated with steep lamina cribrosa curvature but with choroidal microvascular
391 dropout. *Sci Rep* 2020;10(1):6761.

- 392 19. Suh MH, Zangwill LM, Manalastas PI, et al. Deep Retinal Layer Microvasculature
393 Dropout Detected by the Optical Coherence Tomography Angiography in Glaucoma.
394 *Ophthalmology* 2016;123(12):2509-18.
- 395 20. Suh MH, Zangwill LM, Manalastas PIC, et al. Deep-Layer Microvasculature Dropout by
396 Optical Coherence Tomography Angiography and Microstructure of Parapapillary
397 Atrophy. *Invest Ophthalmol Vis Sci* 2018;59(5):1995-2004.
- 398 21. Han JC, Choi JH, Park DY, Lee EJ, Kee C. Border Tissue Morphology Is Spatially
399 Associated with Focal Lamina Cribrosa Defect and Deep-Layer Microvasculature
400 Dropout in Open-Angle Glaucoma. *Am J Ophthalmol* 2019;203:89-102.
- 401 22. Rao HL, Sreenivasaiah S, Dixit S, et al. Choroidal Microvascular Dropout in Primary
402 Open-angle Glaucoma Eyes With Disc Hemorrhage. *J Glaucoma* 2019;28(3):181-87.
- 403 23. Park HL, Kim JW, Park CK. Choroidal Microvasculature Dropout Is Associated with
404 Progressive Retinal Nerve Fiber Layer Thinning in Glaucoma with Disc Hemorrhage.
405 *Ophthalmology* 2018;125(7):1003-13.
- 406 24. Kim CY, Lee EJ, Kim JA, Kim H, Kim TW. Progressive retinal nerve fibre layer thinning
407 and choroidal microvasculature dropout at the location of disc haemorrhage in
408 glaucoma. *Br J Ophthalmol* 2021;105(5):674-80.
- 409 25. Kwon JM, Weinreb RN, Zangwill LM, Suh MH. Parapapillary Deep-Layer
410 Microvasculature Dropout and Visual Field Progression in Glaucoma. *Am J*
411 *Ophthalmol* 2019;200:65-75.
- 412 26. Park H-YL, Kim JW, Park CK. Choroidal microvasculature dropout is associated with
413 progressive retinal nerve fiber layer thinning in glaucoma with disc hemorrhage.
414 *Ophthalmology* 2018;125(7):1003-13.
- 415 27. David RCC, Moghimi S, Do JL, et al. Characteristics of Central Visual Field Progression
416 in Eyes with Optic Disc Hemorrhage. *Am J Ophthalmol* 2021

- 417 28. Jo YH, Kwon J, Jeong D, Shon K, Kook MS. Rapid Central Visual Field Progression
418 Rate in Eyes with Open-Angle Glaucoma and Choroidal Microvasculature Dropout.
419 *Sci Rep* 2019;9(1):8525.
- 420 29. Lee EJ, Kim TW, Kim JA, et al. Elucidation of the Strongest Factors Influencing Rapid
421 Retinal Nerve Fiber Layer Thinning in Glaucoma. *Invest Ophthalmol Vis Sci*
422 2019;60(10):3343-51.
- 423 30. Shin JW, Sung KR, Park SW. Patterns of Progressive Ganglion Cell-Inner Plexiform
424 Layer Thinning in Glaucoma Detected by OCT. *Ophthalmology* 2018;125(10):1515-
425 25.
- 426 31. Anraku A, Enomoto N, Takeyama A, Ito H, Tomita G. Baseline thickness of macular
427 ganglion cell complex predicts progression of visual field loss. *Graefes Arch Clin Exp*
428 *Ophthalmol* 2014;252(1):109-15.
- 429 32. Zhang X, Dastiridou A, Francis BA, et al. Baseline Fourier-Domain Optical Coherence
430 Tomography Structural Risk Factors for Visual Field Progression in the Advanced
431 Imaging for Glaucoma Study. *Am J Ophthalmol* 2016;172:94-103.
- 432 33. Scuderi G, Fragiotta S, Scuderi L, Iodice CM, Perdicchi A. Ganglion Cell Complex
433 Analysis in Glaucoma Patients: What Can It Tell Us? *Eye Brain* 2020;12:33-44.
- 434 34. Lee EJ, Kim JA, Kim TW. Influence of Choroidal Microvasculature Dropout on the Rate
435 of Glaucomatous Progression: A Prospective Study. *Ophthalmol Glaucoma*
436 2020;3(1):25-31.
- 437 35. Kwon J, Shin JW, Lee J, Kook MS. Choroidal Microvasculature Dropout Is Associated
438 With Parafoveal Visual Field Defects in Glaucoma. *Am J Ophthalmol* 2018;188:141-
439 54.
- 440

441 **STATEMENTS**

442 **Acknowledgment/financial support:**

443 National Institutes of Health/National Eye Institute Grants R01EY029058, R01EY011008,
444 R01EY026574, R01EY019869 and R01EY027510; Core Grant P30EY022589; by the donors
445 of the National Glaucoma Research Program (no grant number); a program of the
446 BrightFocus Foundation Grant (G2017122); an Unrestricted Grant from Research to Prevent
447 Blindness (New York, NY); UC Tobacco Related Disease Research Program (T31IP1511);
448 and grants for participants' glaucoma medications from Alcon, Allergan, Pfizer, Merck, and
449 Santen. The sponsor or funding organizations had no role in the design or conduct of this
450 research.

451

452 **Financial Disclosures:**

453 Eleonora Micheletti: none; Sasan Moghimi: none; Takashi Nishida: none; Nevin W. El-
454 Nimri: none; Min H. Suh: none ; James A. Proudfoot: none ; Alireza Kamalipour: none ;
455 Linda M. Zangwill: National Eye Institute (F), Carl Zeiss Meditec Inc. (F), Heidelberg
456 Engineering GmbH (F), OptoVue Inc. (F, R), Topcon Medical Systems Inc. (F, R) Merck
457 (C); Robert N. Weinreb: Allergan (C), Eyenovia (C), Topcon (C), Heidelberg Engineering
458 (F), Carl Zeiss Meditec (F), Konan (F), OptoVue (F), Topcon (F), Centervue (F).

459 **Author Contribution:**

460 Concept design: EM, SM, RNW; Acquisition and reviewing data: TN, SM, NEN, TN, MHS,
461 AK; Analysis or interpretation of data: EM, SM, TN, JAP, LMZ, RNW; Drafting of the
462 manuscript: EM, SM, NEN, RNW; Critical revision of the manuscript: All authors; Obtained
463 funding: SM, LMZ, RNW; Supervision: SM, LMZ, RNW

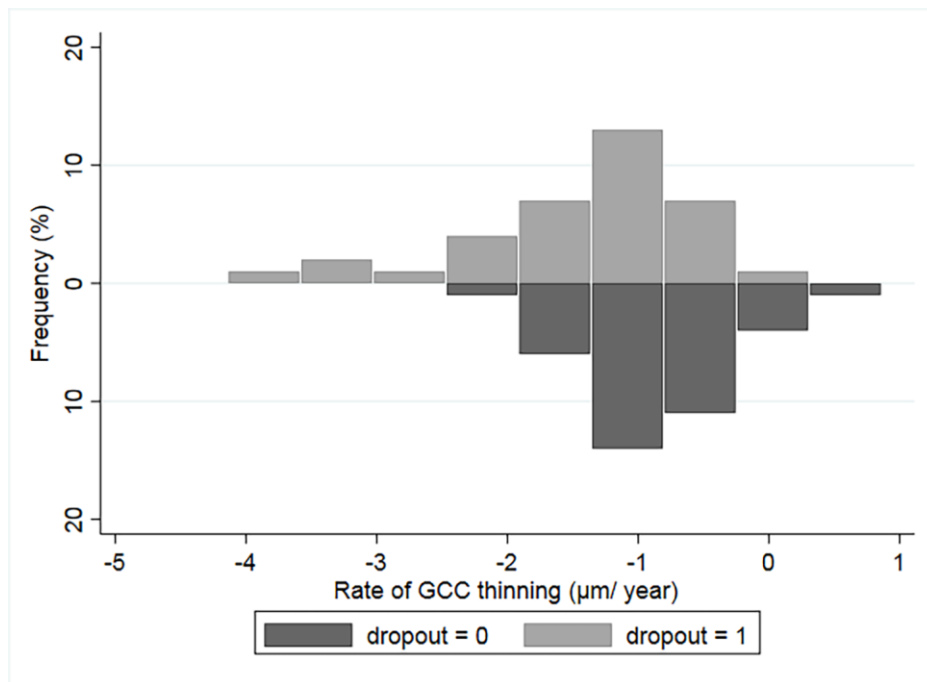
464 **FIGURE LEGENDS**

465

466 Figure 1. OCT-A En-face Choroidal vessel density Map showing supero-temporal MvD
467 (Left) and subsequent hemi-superior GCC thinning (Right) in an open-angle glaucoma eye.

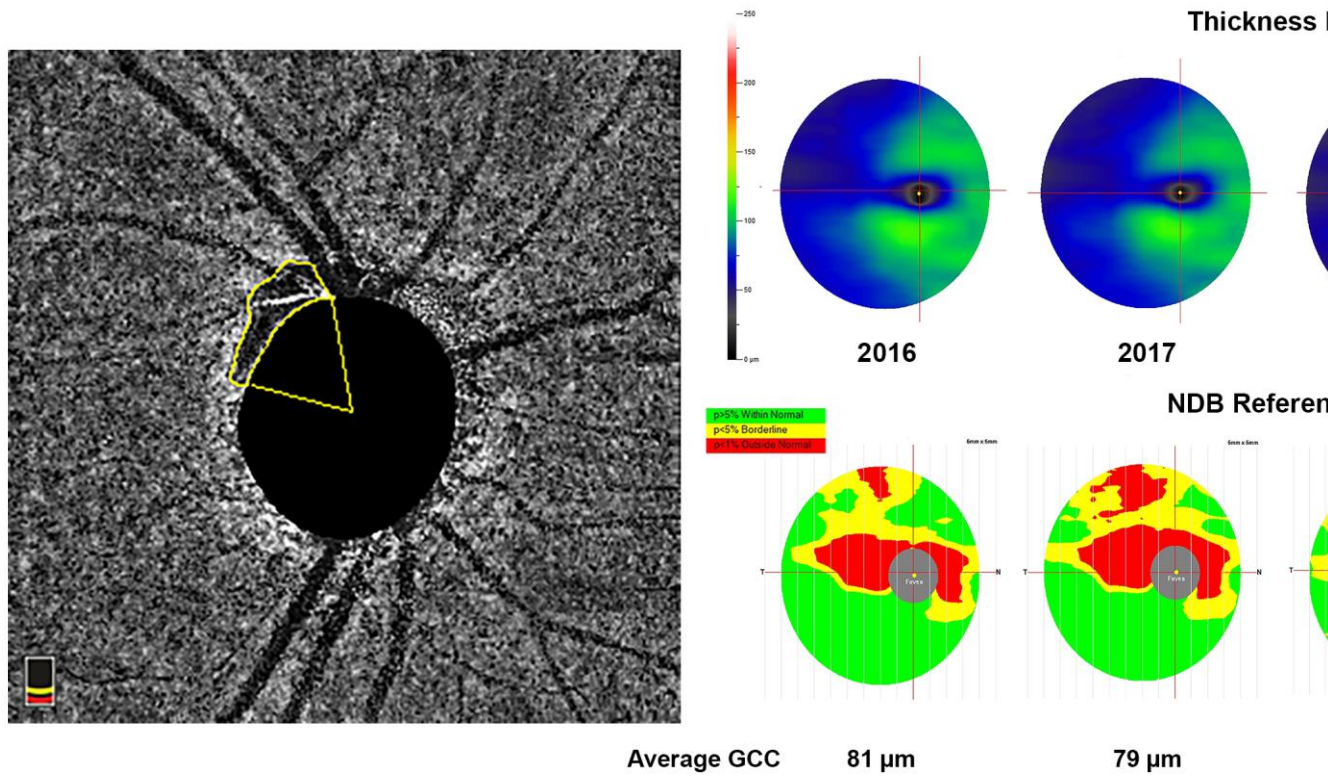
468 OCT-A: Optic Coherence Tomography-Angiography; VD: Vessel Density; MvD: deep-layer

469 Microvascular Dropout; GCC: Ganglion Cell Complex



470
471
472

473 Figure 2. Rates of GCC thinning ($\mu\text{m}/\text{year}$) in eyes with and without deep-layer
474 microvasculature dropout



475